

Implementation of a consistent co-rotational nonlinear dynamic formulation and application to modeling overhead transmission lines

M.C. Vanzulli¹, J.B. Bazzano², G. Usera¹, J.M. Pérez Zerpa²

¹Instituto de Ingeniería Mecánica y Producción Industrial, Facultad de Ingeniería de la Universidad de la República
Julio Herrera y Reissig 565, 11300, Montevideo, Uruguay mvanzulli@fing.edu.uy, gusera@fing.edu.uy

²Instituto de Estructuras y Transporte, Facultad de Ingeniería de la Universidad de la República
Julio Herrera y Reissig 565, 11300, Montevideo, Uruguay
jorgepz@fing.edu.uy, bbazzano@fing.edu.uy

Abstract The overhead transmission lines are frequently affected by severe climate events such as thunderstorms or heavy snowfalls. Such events might cause the disconnection of the line, with potentially severe consequences. In the period of 2000- 2007, more than twenty events of disconnection were registered in one of the main transmission lines in Uruguay. Given the particular features of local winds and temperatures, solutions applied in other countries might not be applicable. This demonstrates the necessity to develop numerical models to enhance the prediction capabilities of these events, guaranteeing in that manner a continuous supply of energy.

The Universidad de la República (UdelaR) counts with research groups working on this problem. The Computational Fluid Mechanics Group (GMFC) is working, since 2004, in the development of computational models of tridimensional fluxes for various applications. The main code developed is called *caffa.3d.MBRi* and it's based on the Finite Volume Method, using MPI parallelization. The group called Modelling and Identification in Solids and Structures (MISES) is committed, since its creation in 2018, to the development of numerical codes for structural analysis. The main code developed is called Open Non-linear Structural Analysis Solver (ONSAS) and it is publicly available.

In this work a reference formulation for consistent non-linear dynamic analysis of beam structures using a co-rotational approach is implemented in the ONSAS code. The authors are not aware of any other open implementation of this formulation available. The implementation is validated using reference problems and also applied to the modelling of high voltage transmission lines considering realistic geometries and loadings.

Keywords: Co-rotational finite element; Overhead transmission lines; Non-linear dynamics; Non-linear analysis; Thunderstorms; Downburst winds.

1 Introduction

Over the last years, thunderstorms caused several damages and service interruptions to the Uruguayan transmission lines system. These downburst nonsynoptic winds can generate excessive oscillations of the conductors. If wind velocity reaches extreme values, the isolator chain can hit the tower, damaging the components or causing service interruptions.

Flexible beam models are applied in vast fields of engineering: such as aircraft industry, propulsion turbines, onshore and offshore windmills. These components behaviour is usually modelled using geometric non-linearity for large displacements. Besides the classic "Updated" (UL) and Total Lagrangian (TL) formulations, they are able to correctly represent wide amplitude movements. On the other hand, thunderstorms caused several damages into Uruguay transmission lines system. This work advances the development of a numerical model capable of predicting the effect of sever thunderstorms onto transmission lines, in order to analyze possible mitigation measures.

On the specific subject of mechanical behaviour of stranded conductors, the doctoral thesis of Foti [1] is remarkable for his detailed analysis using 3D corrotational beam elements. Experimental and numerical studies have shown discrepancies, caused by two factors, the angular updates by incremental approaches and the inherent behaviour of the system. In later works by the same author, the limitations are rectified. The internal sliding of the strands, and their implication of hysteresis phenomenon are modelled in Foti and Martinelli [2]. A 2D dynamic

45 corrotational formulation was published in [3], cooperatively with static model proposed by Battini and Pacoste
 46 [4], a new 3D non-linear dynamic was developed and released in Le et al. [5]. These article is the central reference
 47 of this work. The results provided by the formulation when applied to conductors forced by thunderstorms is still
 48 not fully studied, being the main objective of the present work.

49 The main attractive of the corrotational formulation is the versatility of using different local formulations,
 50 and being able to easily add different types of elements. Additionally the use of this formulation enables to
 51 the decoupling of non-linearities, since the rigid component of the element considers geometric non-linearities
 52 while the deformable component incorporates material non-linearity. Due to these advantages, this methodology
 53 is implemented in many areas of engineering application. The robustness and the versatility of these model is
 54 a significant attractive for different researchers. Co-rotational formulations can be easily included in Open Finite
 55 Element softwares for structural analysis. The library called *Open Nonlinear Structural Analysis Solver* (ONSAS),
 56 was initially presented in [6] as a set of GNU-Octave [7] for research/teaching purposes. A co-rotational formulation
 57 for static analysis of beam structures was recently implemented and validated. In this work we present the results
 58 obtained after the inclusion of the dynamic analysis formulation.

59 In this work the results ONSAS which is capable of modelling the effects of sever winds on the conductor is
 60 presented. In Section 2, the numerical method is detailed, based on the co-rotational formulation presented in Le
 61 et al. Le et al. [5]. In section 3, two numerical applications are presented. The first of these aims to validate the
 62 implementation. This problem in section 3.1, is a classic example in corrotational literature and results presented
 63 are according to Le et al. [5]. Afterwards, a simplified application of a conductor is implemented the line geometry
 64, the wind profile and geometry were extracted from Stengel et al. [8]. Finally, the main results of this article are
 65 summarized in the section 4. In addition, possible future works and their potential are evaluated.

66 2 Methodology

67 2.1 Co-rotational formulation

68 The corrotational method for binodal 3D beam elements is based on the composition of a rigid movement,
 69 which includes large rotations and displacements, superimposed on a deformable solid movement. To understand
 70 this analysis, a series of consecutive rotations illustrated in Fig. 1 must be understood. In Figure 1, it is shown the
 71 assignment of the element on the reference to undeformed configuration. In addition, 1 illustrates the vectors and
 72 frameworks required to locate the element on any configuration.

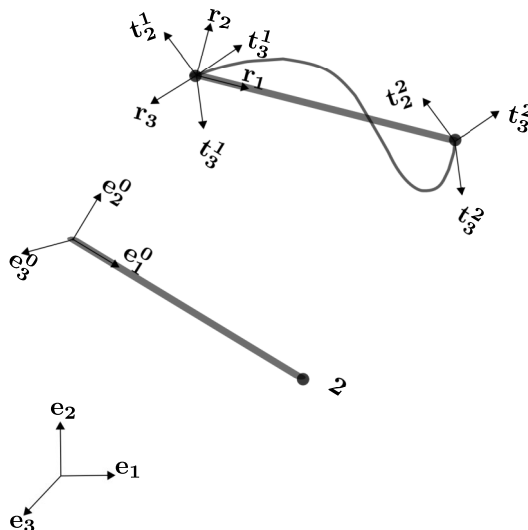


Figure 1. Different configurations defined by corrotational formulation.

73 In this section, the most relevant variables are succinctly presented. First, a global reference system is defined
 74 by the orthogonal base (e_1, e_2, e_3) . Alongside to the element, a framework that moves and rotates solidarity is
 75 defined, denoted by the base (r_1, r_2, r_3) . To locate the element on the undeformed and deformed configuration,
 76 the following triads are set : (e_1^0, e_2^0, e_3^0) and (t_1^1, t_2^1, t_3^1) . The global degrees of freedom (dofs) associated to the
 77 element are: the nodal linear displacements u_i^g and the angular displacements w_i^g . For the local coordinates,

78 the degrees of freedom are reduced to seven, the nodal displacements is replaced by the axial extension of the rod
 79 $u = u = l_n - l_0$ where length in the deformed (l_n) and reference configuration (l_0). Secondly the angles are
 80 transformed to local coordinates.

81 A concise description of the procedure to derive internal and inertial force vector and their corresponding
 82 tangent matrices according to Le et al. [5] and Battini and Pacoste [9]. Considering the kinematic variables defined
 83 in 2.1 in combination with the local displacements, the force vectors and the tangent matrices for these coordinates
 84 are obtained. Then it is necessary to express them in terms of global coordinates. This conversion is calculated by
 85 the matrix \mathbf{B} as expressed in eq. (1).

$$\delta \mathbf{d}_l = \mathbf{B} \delta \mathbf{d}_g \quad \mathbf{f}_l = \mathbf{B}^T \mathbf{f}_g. \quad (1)$$

86 Applying the same methodology described in the previous paragraphs and using auxiliary variables defini-
 87 tions, the expression for the internal force vector and its tangent matrix is presented in global coordinates eq. (2) y
 88 eq. (3).

$$\mathbf{F}^g = \begin{bmatrix} \mathbf{r} \\ \mathbf{P}\mathbf{E}^T \end{bmatrix} \mathbf{f}_a \quad (2)$$

$$\mathbf{K}^g = \mathbf{B}_a^T \mathbf{k}_a \mathbf{B}_a + \mathbf{D}\mathbf{f}_{a1} - \mathbf{E}\mathbf{Q}\mathbf{G}^T\mathbf{E}^T + \mathbf{E}\mathbf{G}\mathbf{a}_r \quad (3)$$

89 With the algebraic aid of the auxiliary matrices \mathbf{G} and \mathbf{E} , the matrix \mathbf{P} link differentials local rotations ($\delta \bar{\mathbf{w}}_1$,
 90 $\delta \bar{\mathbf{w}}_2$) with the global \mathbf{d}_g . Analogously the vector \mathbf{r} contains \mathbf{e}_1 is transformed into global coordinates.

91 Similarly, the matrix \mathbf{B}_a permit to change local coordinates from $\delta \mathbf{d}_a$ to $\delta \mathbf{d}_g$, the term \mathbf{k}_a represents the
 92 contribution into local coordinates. On the other hand, the matrix \mathbf{D} is non-symmetric and is calculated according
 93 to the internal products of the base vectors \mathbf{e}_i , this term provides the stiffness according to the axial force f_{a1} . In
 94 addition, in eq. (3) the matrix \mathbf{Q} is computed multiplying \mathbf{P} and the nodal moments in global coordinates.

95 Now a date, according to the author's knowledge Le et al. [5], any commercial software uses corrotational
 96 formulations for the resolution of dynamic problems.

97 2.2 Wind effect modelling

98 The wind flow is assumed unidirectional on a component transversal to the conductor axis. Although in this
 99 work, the fluctuating component is neglected to mean velocity. Considering air as Newtonian fluid ρ the density
 100 of air only depends on temperature and pressure, C_d the drag coefficient is a function of Reynolds, then the mean
 101 force in the direction of flow ("drag") for diameter d_c and length l_e element is calculated according to eq. (4):

$$F_v = \frac{1}{2} \rho(T) C_d(Re) d_c u_m^2 l_e \quad (4)$$

102 Lift force, on a perpendicular direction to the flow, is considered negligible to drag force. This simplification
 103 is also accompanied by the largest stiffness of the cable on these direction, in addition the weight opposes to
 104 lift force. Moreover, velocities of the element are insignificant respect to storm flow. These hypothesis and the
 105 parameters were extracted from Stengel et al. [8].

106 3 Numerical Results

107 All the simulations were performed using a desktop computer with an intelCorei5 and 16 Gigs of RAM
 108 memory. The ONSAS code ¹ was used, is executed by GNU-Octave [7] and the visualization using the software
 109 Paraview [10].

¹<https://github.com/ONSAS/ONSAS/tree/development>

110 3.1 Right angle cantilever beam

111 These problem was originally presented in Simo and Vu-Quoc [11] and it is usually considered by the litera-
 112 ture to valid three-dimensional beam element formulations for non-linear dynamic analysis (Albino et al. [12] Le
 113 et al. [5]). This problem is illustrated in 2. It is conformed by two identical right-angled bars, where each member
 114 has a length of $L = 10$ m.

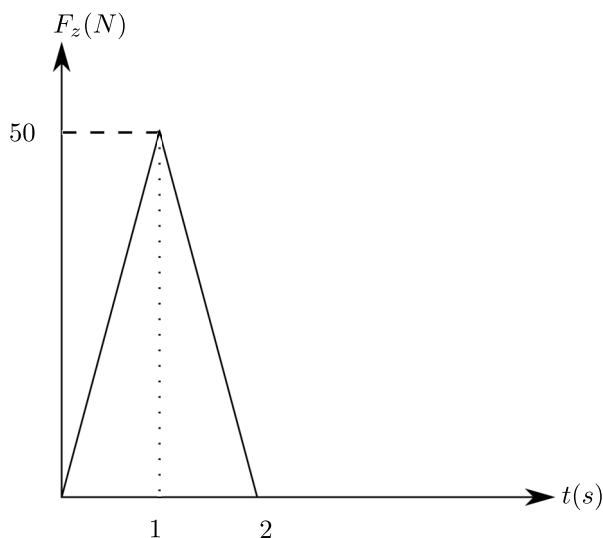
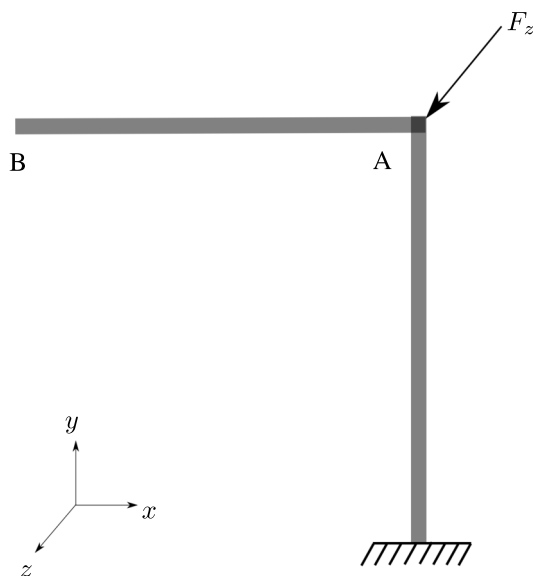


Figure 2. Geometric scheme of right angle cantilever beam example.

Figure 3. Transverse profile force loaded at point A.

115 The material properties must comply certain equals, therefore the choice of these is obtained by solving an
 116 indeterminate compatible system. For this work the second moments of inertia along the axis z and y and the
 117 values of the linear and transverse modulus of elasticity were chosen $E = G = 10^6$ $A = 1$ $I = J = 10^{-3}$ and
 118 $\nu = 0.3$. These values were obtained from the following equations: $GA = EA = 10^6$ and $GJ = EI = 10^3$.

119 The structure is embedded at the base and a force in z direction is applied at the elbow. This force bends
 120 and troses the system into the xy plane, producing free vibrations of wide amplitude. The profile of this force is
 121 illustrated in 3. It acts during two initial seconds, increases linearly until the first second of simulation and then
 122 decreases to zero. The resultant amplitudes generated by this load are of the same magnitude as the dimensions of
 123 the structure. To capture this behaviour 10 elements were chosen by member and a time increment $\Delta T = 0.25$ s.

124 In order to validate this problem, certain degrees of freedom of node A are plotted. These are: the vertical
 125 displacement (according to the y axis) and the transversal displacement (according to z), are illustrated in 4 y 5
 126 respectively. In these, it can be observed that displacements are similar to the dimensions of the structure, so
 127 a free oscillation movement of great amplitude is represented. Analysis of the Figure 4 shows that the sign of
 128 these magnitude is negative during the simulation period. This is linked to the direction of the force applied and
 129 is consistent with the “real” response expected. Both displacements reflect similar behaviour to the results in the
 130 reference literature. The numerical method implemented is an HHT algorithm was used with a value of $\alpha = -0.05$.

131 3.2 Simplified transmission line

132 This section contains a simplified model of the main problem faced by this study. The example is a conductor
 133 of $L_c = 40$ m length with a solid circular cross section of diameter $d_c = 10$ cm. It is conformed by a material with
 134 modulus of elasticity $E = 70$ GPa, modulus of poisson $\nu = 0.3$ and a density similar to conventional aluminium
 135 with $\rho = 2100$ kg/m³.

136 In addition, two insulating chains sustain the cable in vertical position, with a $L_a = 5$ m length each one,
 137 both was considered with identical properties to the cable. These elements are restricted at the atchment point. For

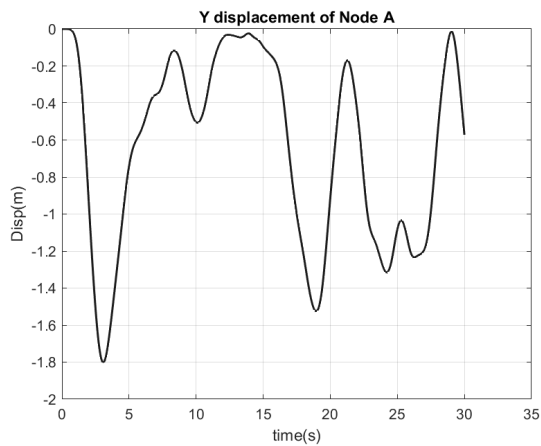


Figure 4. Vertical displacements y of A.

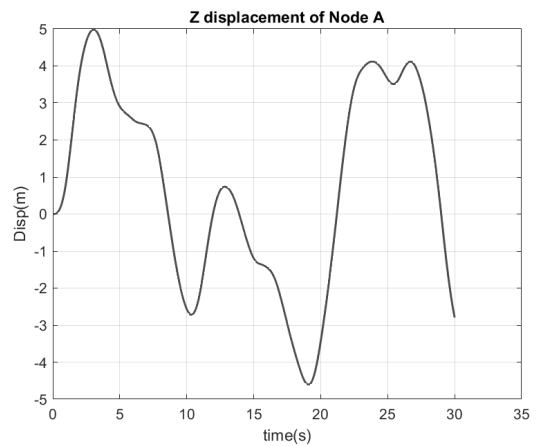


Figure 5. Transversal displacement z of A.

138 the model, a null axial displacement restriction was considered in x and also zero angular displacement in z at the
 139 points C and B . These boundary conditions represent the geometric constraints of the symmetric problem. Another
 140 adjacent span is extended, therefore the axial and angular displacements at the extreme of the spans must be zero.
 141 The geometry of the problem is illustrated in Figure 7.

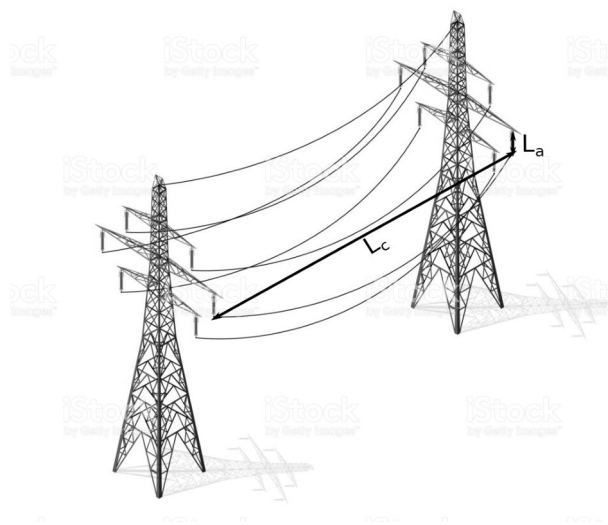


Figure 6. Illustrative scheme of the transmission line system.

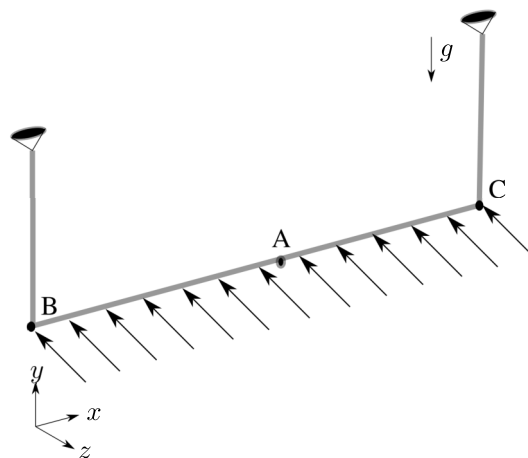


Figure 7. Simplified model.

142 The simulation splits into two stages. First, gravity is applied along the $-z$ axis as shown in the Figure 7.
 143 This mitigates potential instabilities when the element normals tends to zero. After the system response has been
 144 stabilised by the damping, a force according to the z -axis corresponding to the convective storm profile of Stengel
 145 et al. [8] is applied. Spatial fluctuations on the profile along axial coordinate of the cable is not taken into account.
 146 The nodal force in the z -axis is shown in Figure 8 :

147 The vertical and horizontal displacements of A node are plotted below. These figures reveal an inertial behav-
 148 ior and a relationship between the force and displacements profile . This homologous evolution in time between
 149 both magnitudes, responds to an argument based on the Fourier analysis, where the transfer function of the system
 150 offset both variables. In 10 and 9 the vertical and transversal displacements are illustrated respectively.

151 In Figure 11, deformations were plotted for different times. The motion represents the nature of the problem,

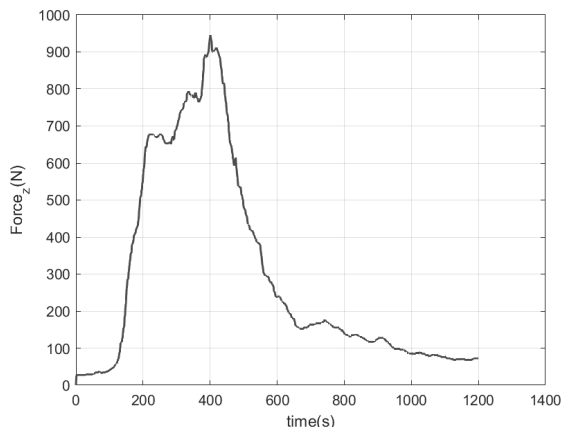


Figure 8. Downburst force in z .

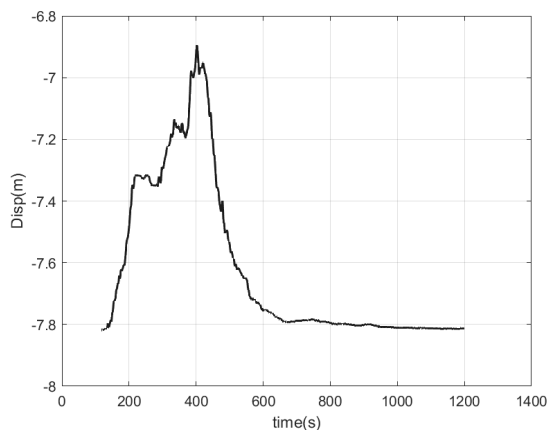


Figure 9. Vertical displacement y of A node

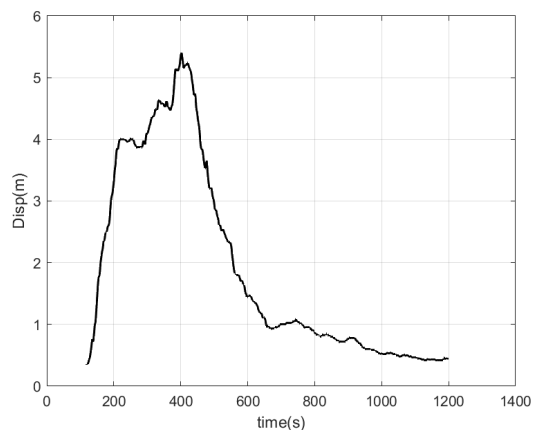


Figure 10. Transversal displacement z of A node

152 and makes explicit the cable’s oscillation, as the forces increase they can compromise the distribution system by
 153 hitting the tower.

154 **4 Conclusions**

155 A consistent, robust and effective corrotational model was implemented and validated being capable to cap-
 156 ture and reproduce large amplitude displacements with a reduced number of elements. This formulation was
 157 specifically applied to high voltage transmission lines loaded by wind profiles extracted from recent articles on the
 158 subject [8]. The system’s responses denotes the excessive sway angle of the conductor 11, related to this type of
 159 loads, the codes developed can be used as a complementary analysis tool for the design of power transmission sys-
 160 tems. Connecting 9 and 8, the identical shape of both profiles can be observed, fulfilling the expectations. Future
 161 works, should verify the non internal slip as published in Foti and Martinelli [2]. This hysteresis behaviour depends
 162 on the normal forces within the cable, this is essential to ensure the correct modelling of the conductor as a circular
 163 solid. Another eventual possible future work, it is possible to implement a model coupled with the tower, where
 164 the displacements of the attachment point and the resonance frequencies of the tower are not neglected. Finally,
 165 it is worth highlighting the potential of this work to develop an integrated solver between the ONSAS-CAFFA
 166 software presented in Usera et al. [13]

167

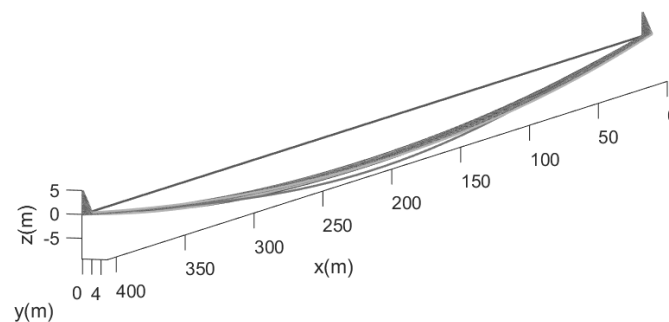


Figure 11. Deformations history of the cable.

References

- [1] Foti, F., 2013. *A corotational beam element and a refined mechanical model for the nonlinear dynamic analysis of cables*. PhD thesis, Doctoral Dissertation, Politecnico di Milano, Milan (Italy).
- [2] Foti, F. & Martinelli, L., 2018. Finite element modeling of cable galloping vibrations—part i: Formulation of mechanical and aerodynamic co-rotational elements. *Archive of Applied Mechanics*, vol. 88, n. 5, pp. 645–670.
- [3] Le, T. N., Battini, J. M., & Hjiij, M., 2011. Efficient formulation for dynamics of corotational 2D beams. *Computational Mechanics*, vol. 48, n. 2, pp. 153–161.
- [4] Battini, J. M. & Pacoste, C., 2002a. Co-rotational beam elements with warping effects in instability problems. *Computer Methods in Applied Mechanics and Engineering*, vol. 191, n. 17-18, pp. 1755–1789.
- [5] Le, T.-N., Battini, J.-M., & Hjiij, M., 2014. A consistent 3d corotational beam element for nonlinear dynamic analysis of flexible structures. *Computer Methods in Applied Mechanics and Engineering*, vol. 269, pp. 538–565.
- [6] Bazzano, J. B. & Pérez Zerpa, J., 2017. *Introducción al análisis no lineal de estructuras*.
- [7] Eaton, J. W., Bateman, D., Hauberg, S., & Wehbring, R., 2019. *GNU Octave version 5.1.0 manual: a high-level interactive language for numerical computations*.
- [8] Stengel, D., Thiele, K., Clobes, M., & Mehdiانpour, M., 2017. Aerodynamic damping of nonlinear movement of conductor cables in wind tunnel tests, numerical simulations and full scale measurements. *Journal of Wind Engineering and Industrial Aerodynamics*, vol. 169, pp. 47–53.
- [9] Battini, J.-M. & Pacoste, C., 2002b. Co-rotational beam elements with warping effects in instability problems. *Computer Methods in Applied Mechanics and Engineering*, vol. 191, n. 17-18, pp. 1755–1789.
- [10] Squillacote, A. H., Ahrens, J., Law, C., Geveci, B., Moreland, K., & King, B., 2007. *The paraview guide*, volume 366. Kitware Clifton Park, NY.
- [11] Simo, J. C. & Vu-Quoc, L., 1988. On the dynamics in space of rods undergoing large motions—a geometrically exact approach. *Computer methods in applied mechanics and engineering*, vol. 66, n. 2, pp. 125–161.
- [12] Albino, J. C. R., Almeida, C. A., Menezes, I. F. M., & Paulino, G. H., 2018. Co-rotational 3D beam element for nonlinear dynamic analysis of risers manufactured with functionally graded materials (FGMs). *Engineering Structures*, vol. 173, pp. 283–299.
- [13] Usera, G., Vernet, A., & Ferré, J., 2008. A parallel block-structured finite volume method for flows in complex geometry with sliding interfaces. *Flow, Turbulence and Combustion*, vol. 81, n. 3, pp. 471.